Electronic Supplementary Information

Electrocatalytic hydrogen evolution reaction with a Cu porphyrin bearing *meso*-CF_3 substituents

Wenzi Li, Xinyang Peng,* Haonan Qin, Yuhan Xu, Jinxiu Han, Haitao Lei and Rui Cao*

Key Laboratory of Applied Surface and Colloid Chemistry, Ministry of Education, School of Chemistry and Chemical Engineering, Shaanxi Normal University, Xi'an 710119, China.

Correspondence E-mail: pengxinyang@snnu.edu.cn, ruicao@snnu.edu.cn

General Materials and Methods.

Manipulations of air- and moisture-sensitive materials were performed under N_2 gas using standard Schlenk line techniques. Reagents used in this work were purchased from commercial suppliers and were used directly without further purification unless otherwise stated. Cu porphyrin **2** was synthesized according to the method we reported recently.[1] All solvents used in this work were reagent grades. Dry solvents, including dichloromethane, acetonitrile, chloroform, and methanol were purified by passage through activated alumina. Toluene was refluxed over sodium blocks and was distilled under reduced pressure. All aqueous solutions were prepared freshly using Milli-Q water.

High-resolution mass spectra (HRMS) were acquired using a Brüker MAXIS apparatus. ^{1}H NMR spectra were acquired using JEOL spectrometer operating at 400 MHz. UV-vis spectra were collected using a Hitachi U-3310 spectrophotometer. The H_2 generated during the electrolysis was analyzed by a Shimadzu GC-2014 gas chromatograph. Electron paramagnetic resonance (EPR) spectra were recorded at 100 K using Brüker E500 EPR spectrometer.

Electrochemical Studies.

All electrochemical measurements in this work were tested using a CH instrument (model CHI660E Electrochemical Analyzer). The cyclic voltammograms (CVs) were recorded in acetonitrile containing 0.10 M Bu_4NPF_6 and 0.50 mM catalyst at 20 °C using a three-compartment cell with a glassy carbon (GC) as the working electrode, a graphite as the auxiliary electrode, and a Ag/$AgNO_3$ (BASi, 10 mM $AgNO_3$, 0.10 M Bu_4NPF_6 in acetonitrile) as the reference electrode. The solutions were bubbled with N_2 for 30 min prior to the measurement. The GC electrode was polished with α-Al_2O_3 of decreasing size (1.0 μm to 50 nm) and washed with distilled water and acetonitrile. Ferrocene was added after the measurements as an internal standard. The electrolysis in acetonitrile was performed in a three-compartment electrochemical cell under N_2 using a GC plate (1.0 cm^2) working electrode. The faradaic efficiency (FE) for the H_2 production during the electrolysis was analyzed by injecting 200 μL gas from the headspace of the cell into a gas chromatograph using a gas-tight syringe and was calculated using the following equation:

$$\mathrm{FE}\ (\%) = \frac{nZF}{Q} \times 100\%$$

in which n is the mole of H_2 produced, $Z = 2$ is the number of electrons transferred for H_2, F is the Faraday constant, and Q is the total charges passed during electrolysis.

Calculation of Diffusion Coefficient from CV Measurements.

The diffusion coefficient of **1** and **2** was calculated using the following equation:

$$i_\mathrm{p} = 0.4463(F/RT)^{1/2} n^{3/2} FAD^{1/2} C v^{1/2}$$

in which i_p is the peak current, F is the Faraday constant, R is the gas constant, T is the temperature, n is the number of electrons transferred ($n = 1$ for the $\mathrm{Cu}^{\mathrm{II/I}}$ redox couple), A is the area of the surface of the electrode (0.07 cm^2), D is the diffusion coefficient of the complex, C is the concentration of the complex (0.5 mM), and v is the scan rate used during CV measurements. The diffusion coefficient (D) was calculated from the slope of i_p versus $v^{1/2}$ plot.

X-ray Diffraction Studies.

High-quality single crystals of **1** were obtained by slow evaporation of a methanol and dichloromethane solution of **1** at room temperature under dark. The complete data set of **1** (CCDC 2330533) was collected. The crystal of **1** suitable for X-ray diffraction studies was coated with Paratone-N oil, suspended in a small fiber loop, and placed in a cooled N_2 gas stream at 153(2) K on a Bruker D8 VENTURE X-ray diffractometer. Diffraction intensities were measured using graphite-monochromated Mo Kα radiation ($\lambda = 0.71073$ Å). Data collection, indexing, data reduction and final unit cell refinements were carried out using APEX2.[2] Absorption corrections were applied using the program SADABS.[3] The structures were solved with direct methods using SHELXS[4] and refined against F^2 on all data by full-matrix least squares with SHELXL-97,[5] following established refinement strategies. Details of the data quality and a summary of the residual values of the refinements are listed in Table S1. The X-ray structure of **1** was checked using IUCr's CheckCIF routine, which resulted in no level A and B alerts.

Synthesis of Cu Porphyrin 1.

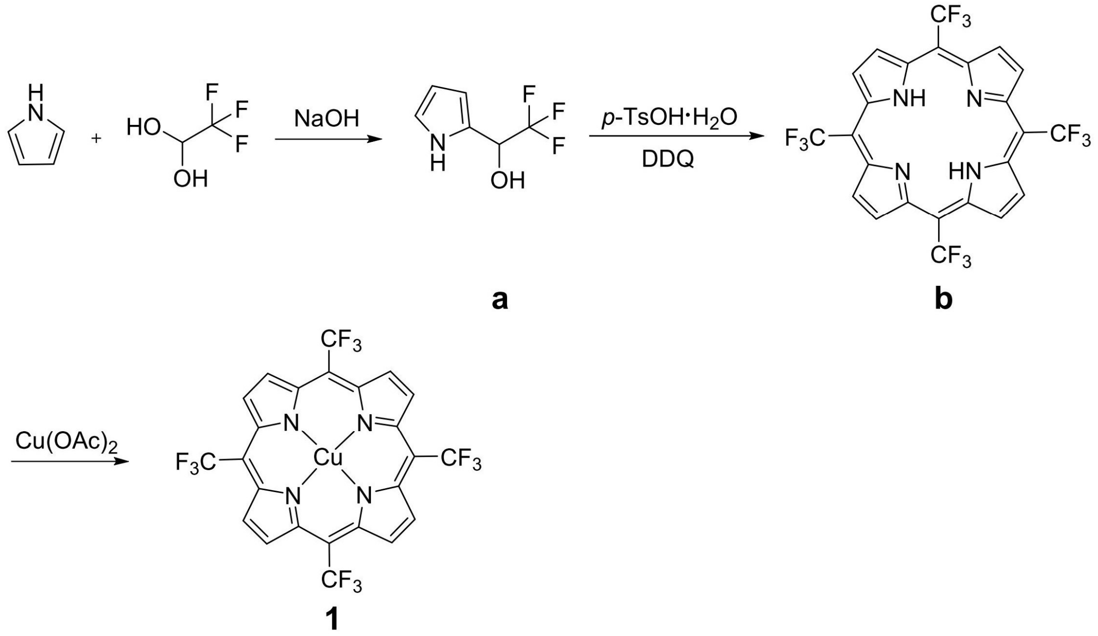

Scheme S1 The synthetic route of Cu porphyrin **1**.

Synthesis of a. To a 25.0 mL oven-dried flask equipped with a stirring bar, was added 5.0 mL trifluoroacetaldehyde hydrate (53.0 mmol). After purging the flask with N_2, 2.0 mL pyrrole (29.0 mmol) and 0.70 g NaOH (17.3 mmol) were added at 0 °C. The solution was then stirred for 4 d under dark. After the reaction was completed, the volatiles were removed by a rotatory evaporator. Then, the crude products were washed with water and was extracted with chloroform. After drying the solution with Na_2SO_4, the solvent was then removed. A tan powder of **a** (1.93 g, yield 40.4%) was afforded after keeping the solution at −20 °C. ^1H NMR ($CDCl_3$) $\delta = 8.53$ (br, 1H), 6.85 (m, 1H), 6.31 (m, 1H), 6.21 (m, 1H), 5.06 (m, 1H), 2.66 (s, 1H) (Fig. S1).

Synthesis of b. To a 500 mL two-necked flask equipped with a magnetic stirring bar and a recycling Dean Stark trap, were added 350 mL dry toluene and 139 mg *p*-toluenesulfonic acid monohydrate (*p*-TsOH·H_2O, 0.73 mmol). The solution was then bubbled with N_2 and refluxed for 2 h under dark. Then, 486 mg **a** (2.93 mmol) was added to the flask. After reacting for 20 min, 1.60 g DDQ (7.03 mmol) was added and the reaction was continued for another 10 min. After the addition of 0.2 mL pyridine, the solution was then cooled to room temperature and was filtered by a crude silica chromatography. The solution with red fluorescence was collected and the solvent was removed by a rotatory evaporator. Purification by another silica chromatography (with hexane) afforded dark purple solids of **b** (113 mg, yield 26.5%). ^{1}H NMR (400 MHz, $CDCl_3$): δ = 9.20 (s, 8H), −2.16 (s, 2H) (Fig. S2). HRMS of $[M+H]^+$: calcd. for $C_{24}H_{11}F_{12}N_4$, 583.0787, found, 583.0790 (Fig. S3).

Synthesis of 1. To a 250 mL flask equipped with a stirring bar, were added 100 mL chloroform and 50.0 mg **b** (0.086 mmol). Then, a 15 mL methanol solution of 513 mg $Cu(OAc)_2·H_2O$ (2.58 mmol) was added into the flask. After refluxing the solution for 3 h under dark, the solvent was then removed by a rotatory evaporator. The crude products were purified through silica chromatography (with hexane) to afford dark purple solids of **1** (48.6 mg, yield 87.7%). HRMS of $[M+H]^+$: calcd. for $C_{24}H_9CuF_{12}N_4$, 643.9926, found, 643.9924 (Fig. S4).

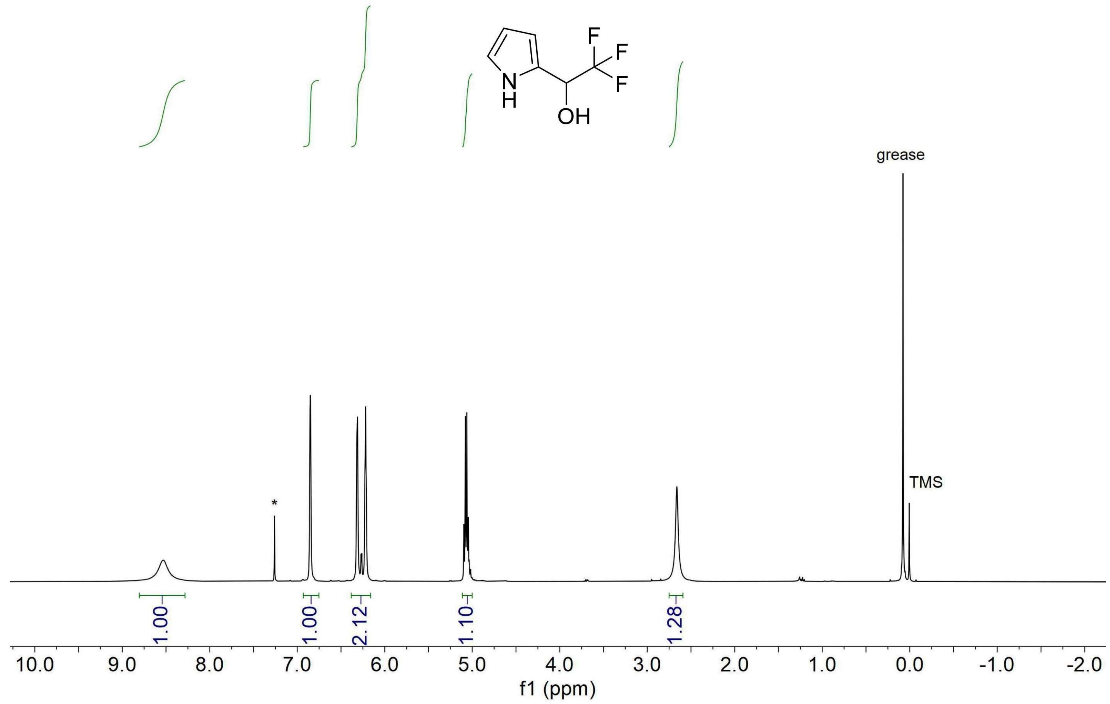

Fig. S1 ^{1}H NMR spectrum of **a** in $CDCl_3$. The solvent residue peak is labeled (*).

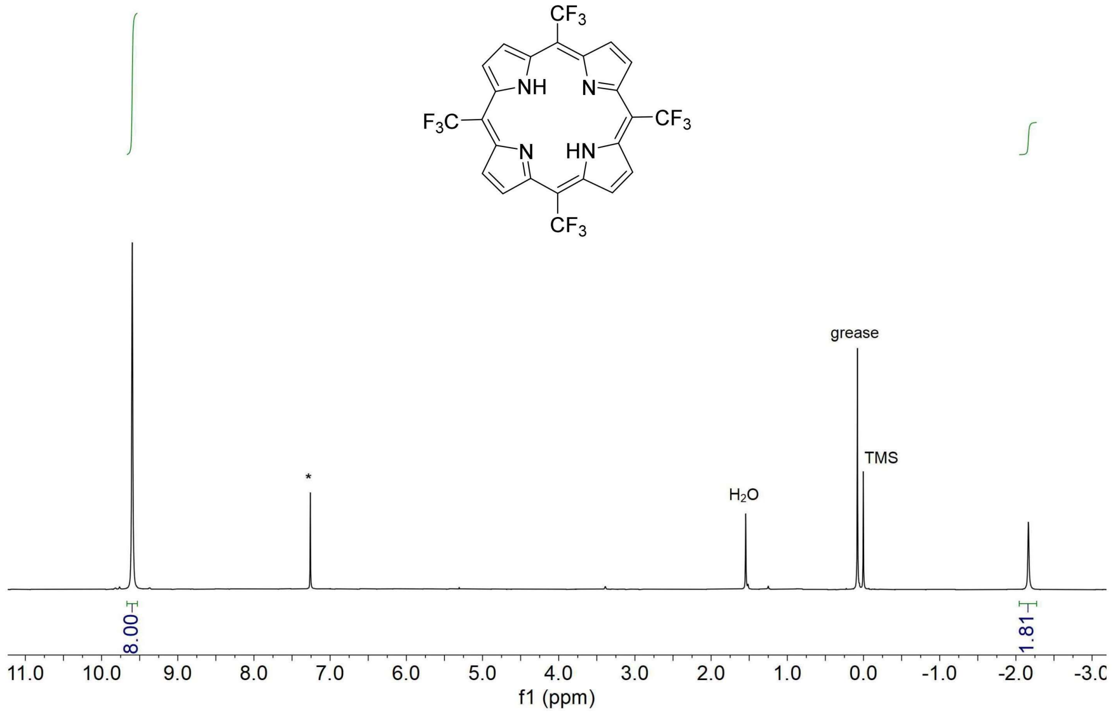

Fig. S2 ^{1}H NMR spectrum of **b** in $CDCl_3$. The solvent residue peak is labeled (*).

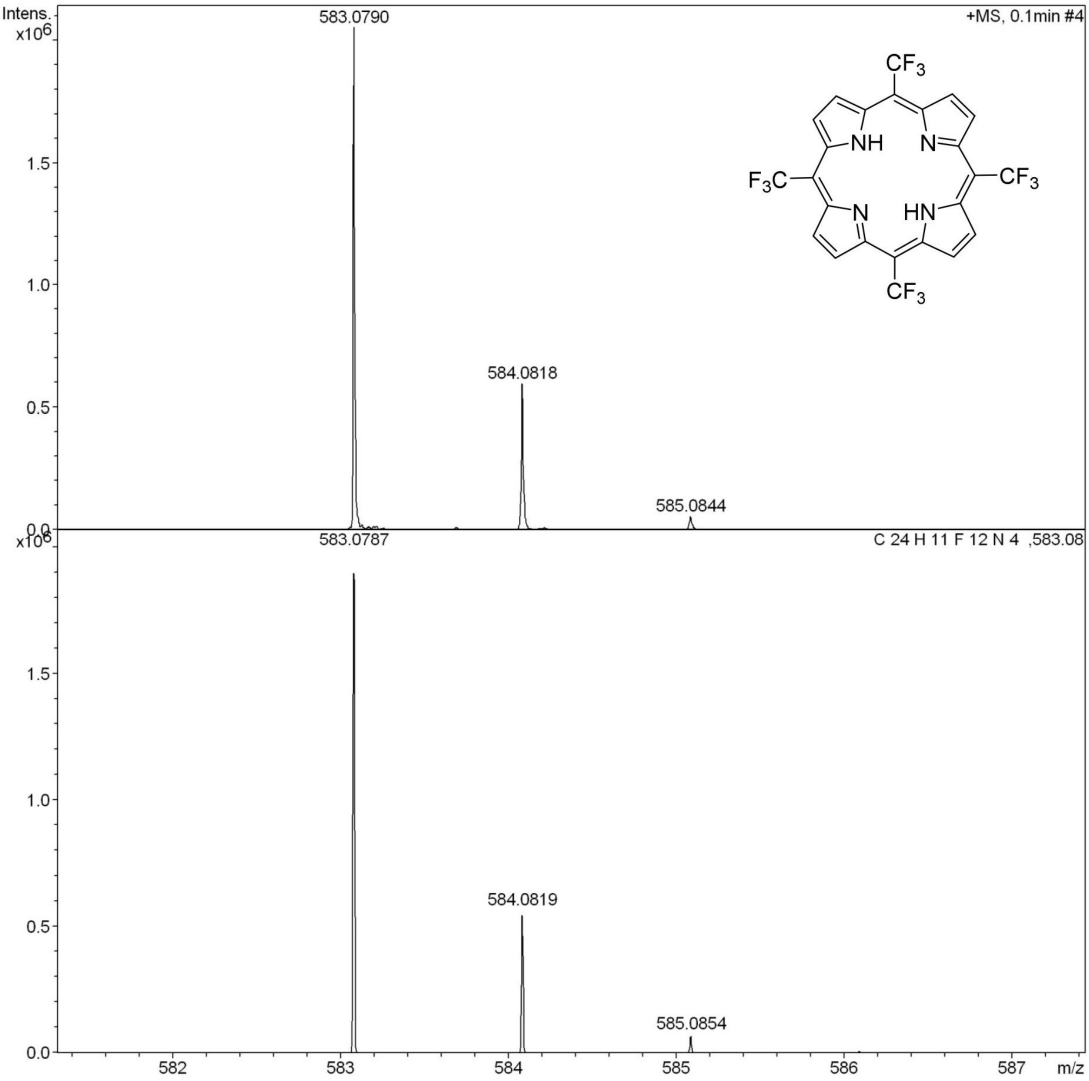

Fig. S3 HRMS of **b** in methanol. The ion at a mass-to-charge ratio of 583.0790 matches the calculated value of 583.0787 for the monocation of $[C_{24}H_{11}F_{12}N_4]^+$.

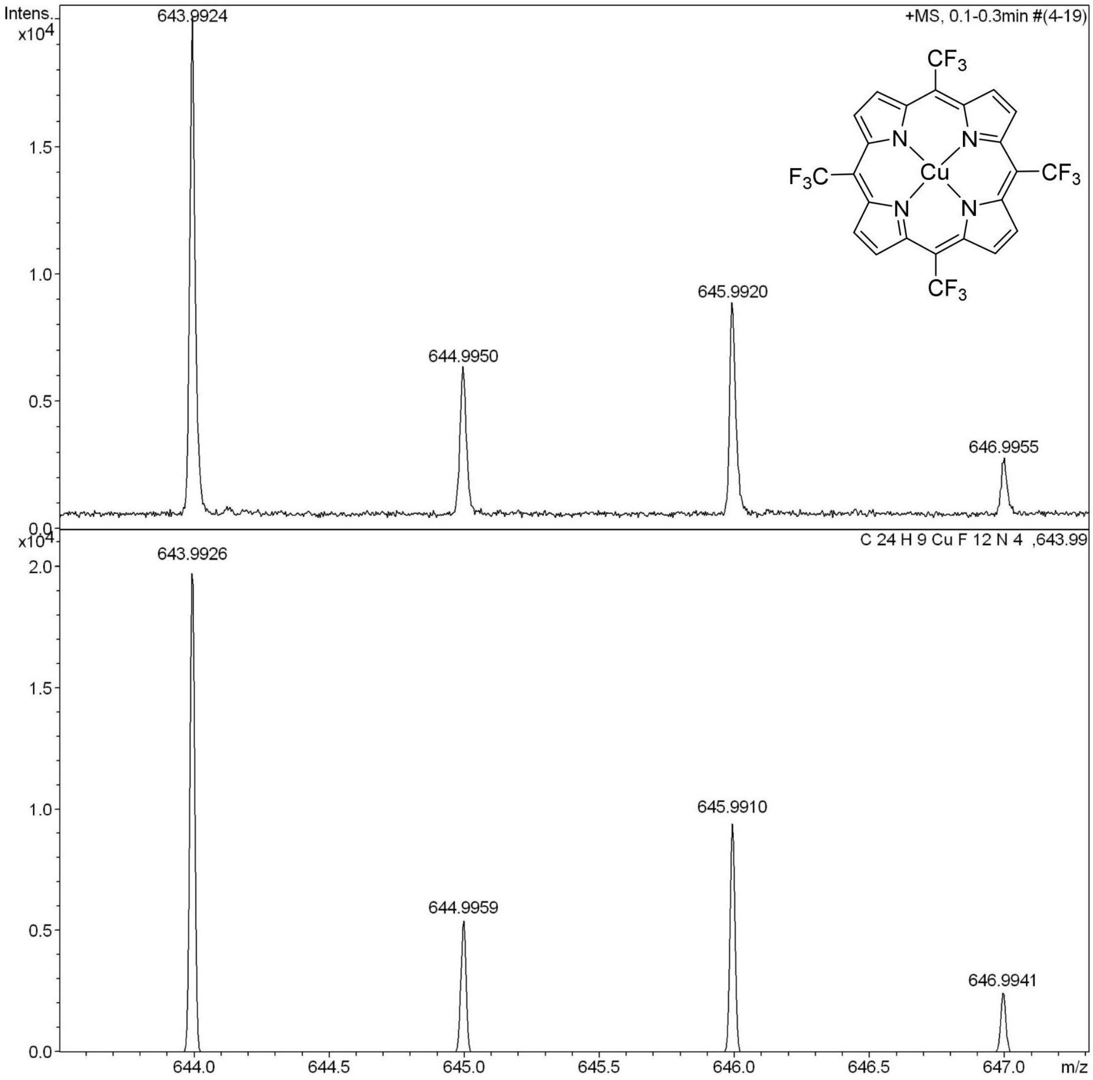

Fig. S4 HRMS of **1** in methanol. The ion at a mass-to-charge ratio of 643.9924 matches the calculated value of 643.9926 for the monocation of $[C_{24}H_9CuF_{12}N_4]^+$.

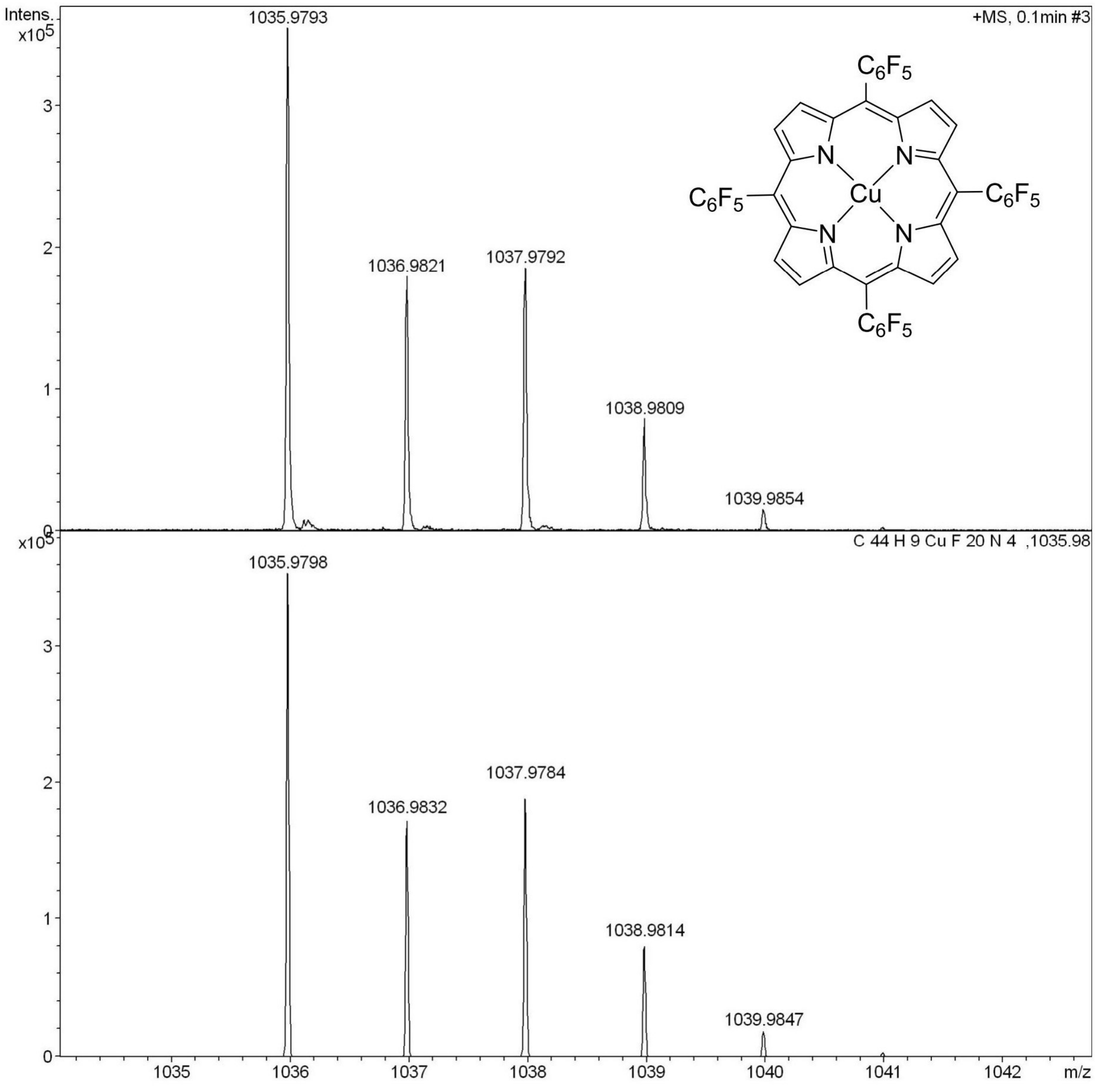

Fig. S5 HRMS of **2** in methanol. The ion at a mass-to-charge ratio of 1035.9793 matches the calculated value of 1035.9798 for the monocation of $[C_{44}H_9CuF_{20}N_4]^+$.

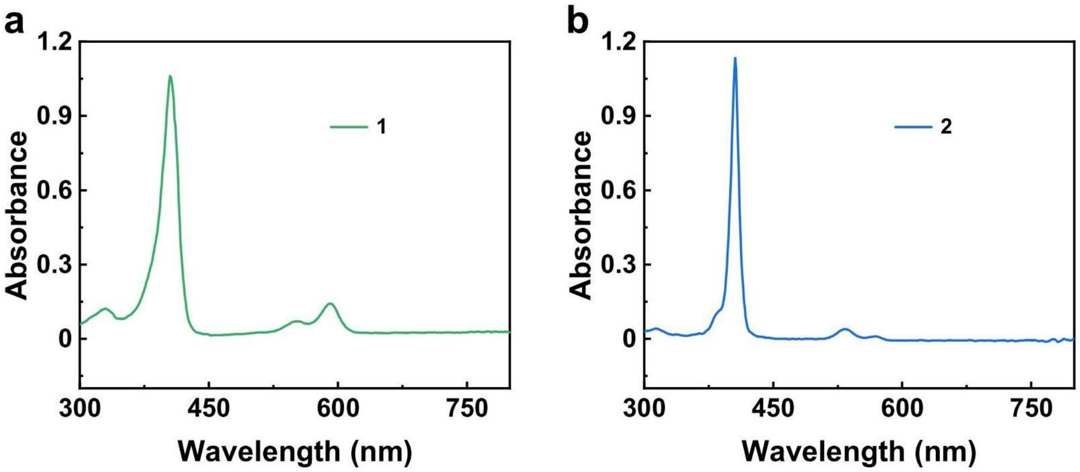

Fig. S6 UV-vis spectra of **1** (a) and **2** (b) in acetonitrile.

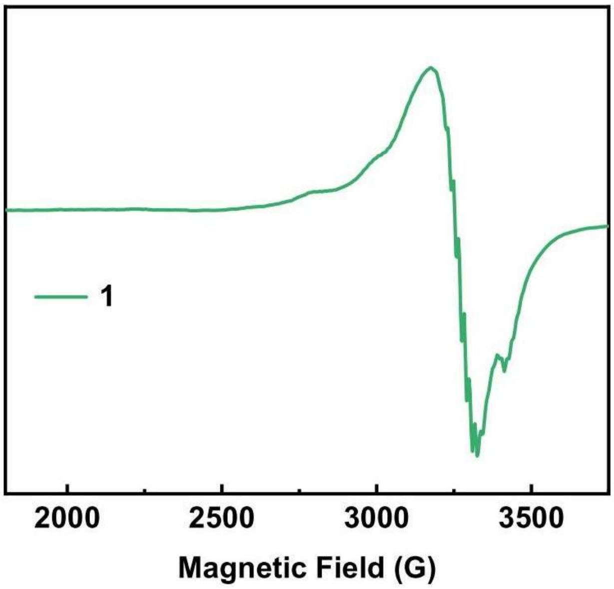

Fig. S7 The EPR spectrum of **1** in acetonitrile at 100 K.

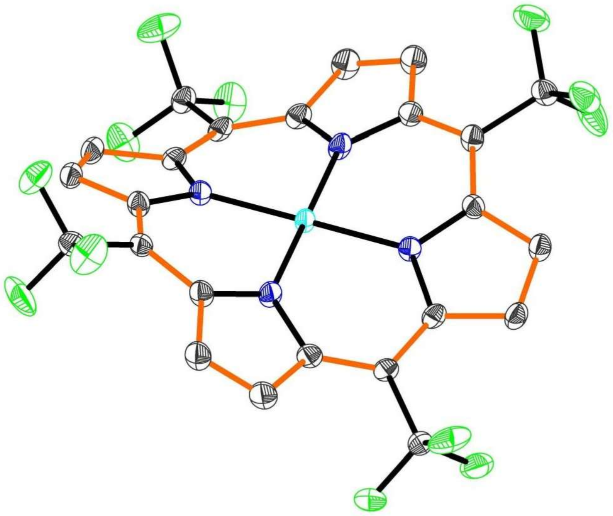

Fig. S8 The thermal ellipsoid plot (30% probability) of the X-ray structure of **1** showing the ruffle sructure. Color code: blue-green, Cu; black, C; blue, N; green, F. Hydrogen atoms are omitted for clarity.

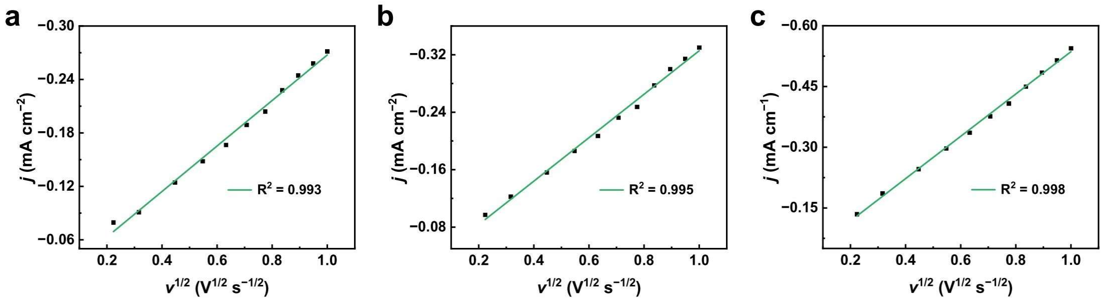

Fig. S9 The reduction peak currents of **1** at −1.00 V (a), −1.33 V (b), and −1.57 V (c) versus the square root of scan rates, giving a diffusion coefficient value of $D_{\mathbf{1}} = 1.51 \times 10^{-5}$ cm^2 s^{-1}.

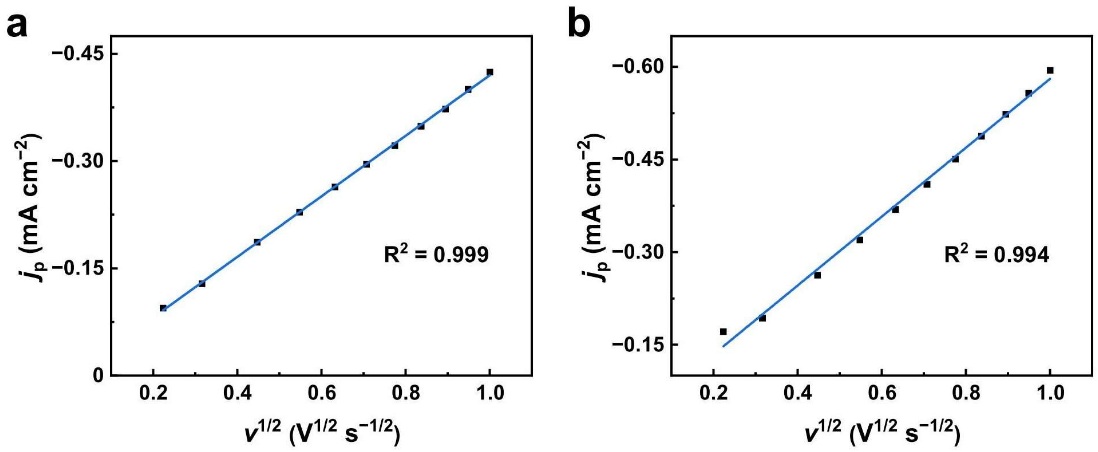

Fig. S10 The reduction peak currents of **2** at −1.30 (a) and −1.75 V (b) versus the square root of scan rates, giving a diffusion coefficient value of $D_{\mathbf{2}} = 9.95 \times 10^{-6}$ cm^2 s^{-1}.

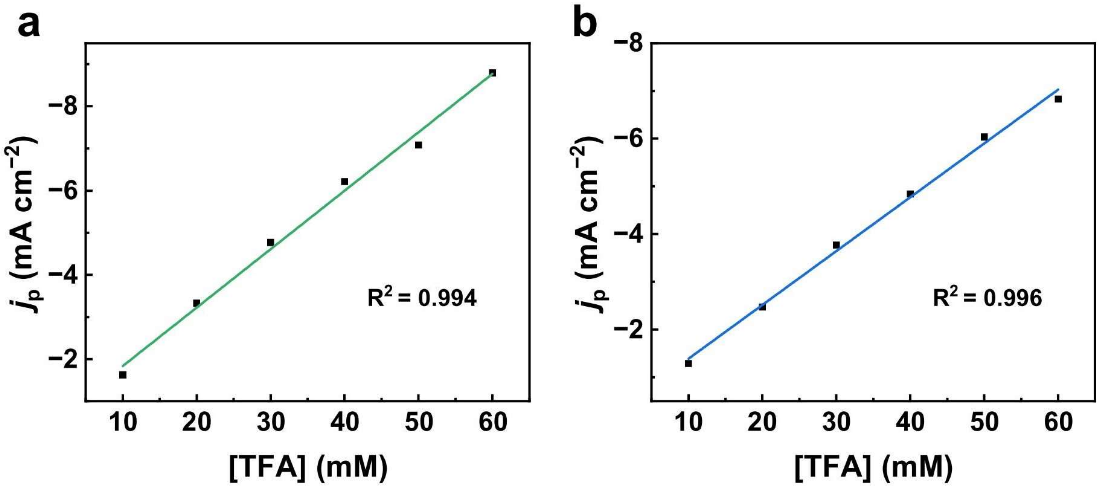

Fig. S11 The plot of catalytic peak current of **1** (a) and **2** (b) versus the concentration of TFA.

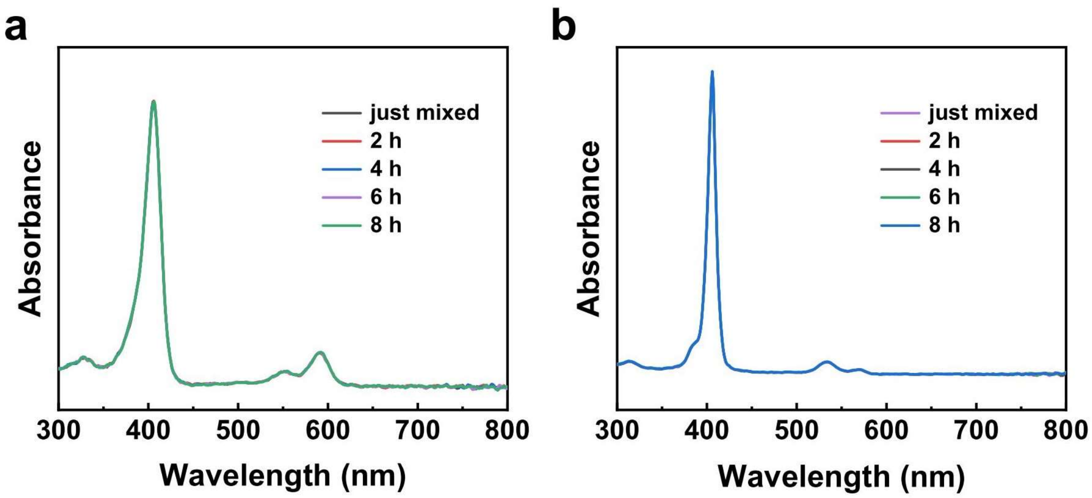

Fig. S12 UV-vis spectra of **1** (a) and **2** (b) in acetonitrile in the presence of 60 mM TFA under dark.

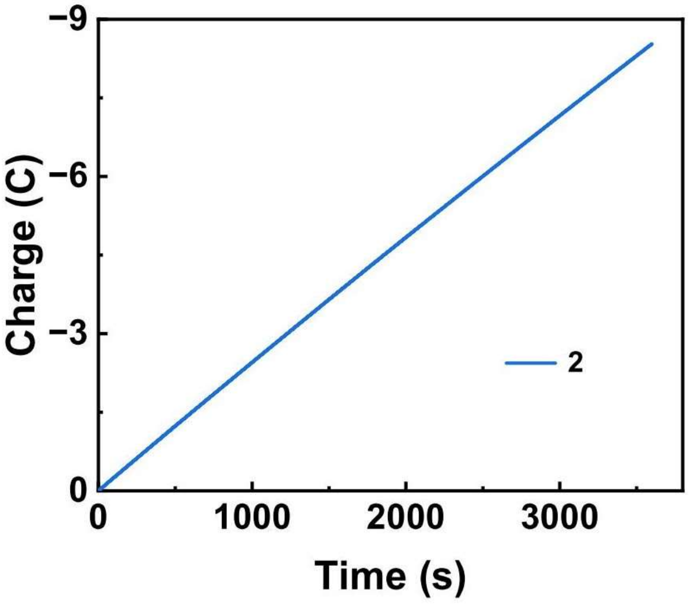

Fig. S13 The electric charge accumulated during the electrolysis with **2** at −1.25 V.

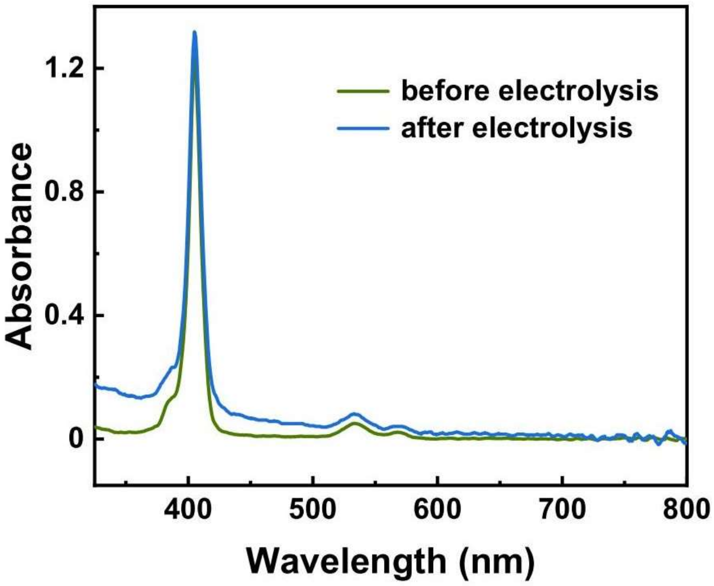

Fig. S14 UV-vis spectra of **2** before and after electrolysis in acetonitrile.

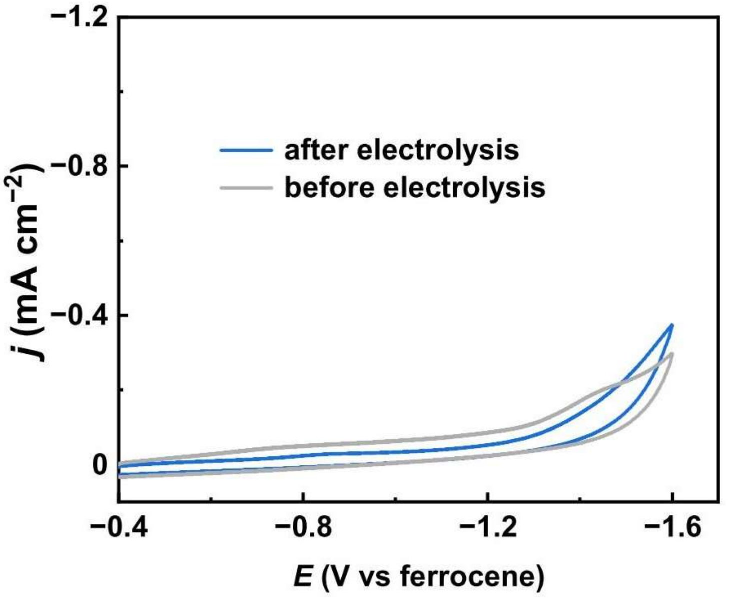

Fig. S15 CVs of the GC working electrode in a TFA-only acetonitrile before and after electrolysis with **2**.

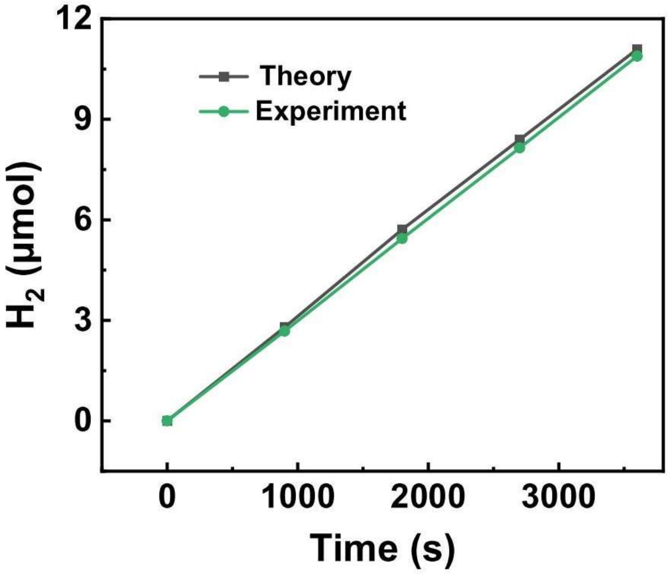

Fig. S16 The detection of evolved H_2 during the electrolysis with **1** at −0.95 V.

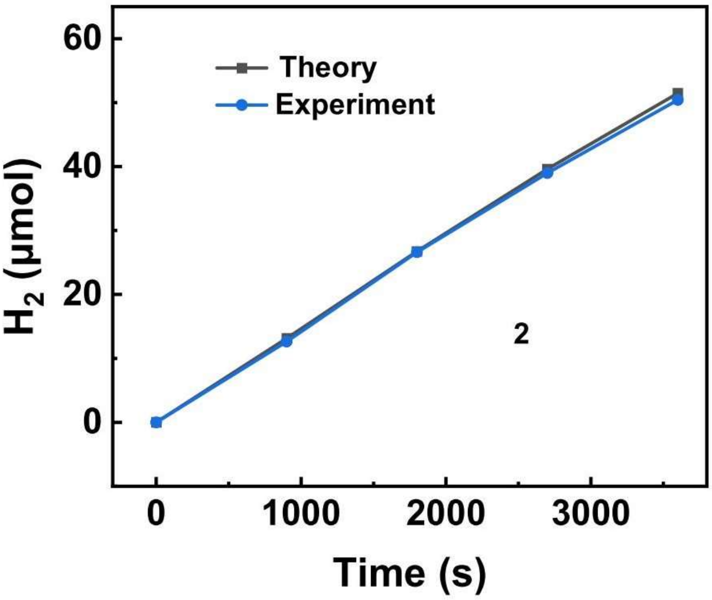

Fig. S17 The detection of evolved H_2 during the electrolysis with **2** at −1.25 V.

Table S1 Crystal data and structure refinement parameters for the X-ray structure of **1**.

Complex	**1**
molecular formula	$C_{24}H_8CuF_{12}N_4$
formula wt. (g mol^{-1})	643.88
temperature (K)	153(2)
radiation (λ, Å)	0.71073
crystal system	Monoclinic
space group	$C2/c$
a (Å)	24.929(4)
b (Å)	4.2898(10)
c (Å)	22.535(4)
β (°)	116.829(9)
volume (Å^3)	2150.5(7)
Z	4
ρ_{calcd} (g cm^{-3})	1.989
μ (mm^{-1})	1.145
F(000)	1268
crystal size (mm^3)	0.20 × 0.10 × 0.10
theta range(°)	2.460 to 26.601
reflections collected	25982
independent reflections	2232 [R(int) = 0.0860]
completeness	99.5%
final R indices	$R_1{}^a = 0.0470$
[$R > 2\sigma$ (I)]	$wR_2{}^b = 0.1245$
R indices (all data)	$R_1{}^a = 0.0483$ $wR_2{}^b = 0.1257$
largest diff. peak and hole (e Å^{-3})	1.274 and −0.996

$^aR_1 = \Sigma||F_o| - |F_c|| / |F_o|$, $^bwR_2 = \{\Sigma[w(F_o{}^2 - F_c{}^2)^2] / \Sigma[w(F_o{}^2)^2]\}^{0.5}$

Table S2 Comparison of electrocatalytic HER onset potentials catalyzed by **1** and molecular electrocatalysts in acetonitrile.

Metal complex	[TFA]	Onset potential (versus ferrocene)	Reference
1	60.0 mM	−900 mV	this work
$(NCHS_2)Ni(OTf)_2$	90.0 mM	−850 mV	6
Ni complex 4	61.1 mM	−1040 mV	7
Compound I	10.0 mM	−1180 mV	8
Ni complex 2c	30.0 mM	−1230 mV	9
$Cu\text{-}Cl_8$	160 mM	−1180 mV	10
$[Ni\text{-}I]_4^0$	200 mM	−960 mV	11
Cu porphyrin 1	60.0 mM	−930 mV	12
2-NBPC-Sb 1	7.60 mM	−980 mV	13
$[Ni(QCl\text{-}tpy)_2]^{2+}$	28.0 mM	−970 mV	14

Supporting References

1 X. Peng, M. Zhang, H. Qin, J. Han, Y. Xu, W. Li, X.-P. Zhang, W. Zhang, U.-P. Apfel and R. Cao, *Angew. Chem. Int. Ed.*, 2024, **63**, e202401074.

2 *APEX2 v2009*, Bruker AXS, Madison, WI, 2009.

3 G. M. Sheldrick, *SADABS*, *2008/1*, University of Göttingen, Göttingen, Germany, 2008.

4 G. M. Sheldrick, *Acta Cryst.*, *Sect. A: Found. Crystallogr.*, 1990, **46**, 467-473.

5 G. M. Sheldrick, *Acta Cryst.*, *Sect. A: Found. Crystallogr.*, 2008, **64**, 112-122.

6 S. Chakrabarti, S. Sinha, G. N. Tran, H. Na and L. M. Mirica, *Nat. Commun.*, 2023, **14**, 905.

7 S. Kaur-Ghumaan, P. Hasche, A. Spannenberg and T. Beweries, *Dalton Trans.*, 2019, **48**, 16322-16329.

8 A. V. Dolganov, T. V. Boykova, A. D. Yudina, L. A. Klimaeva, E. V. Okina and S. G. Kostryukov, *Int. J. Hydrogen Energy*, 2024, **60**, 11-19.

9 S. Xue, X. Lv, N. Liu, Q. Zhang, H. Lei, R. Cao and F. Qiu, *Inorg. Chem.*, 2023, **62**, 1679-1685.

10 K. Sudhakar and P. K. Panda, *ACS Appl. Energy Mater.*, 2022, **5**, 13492-13500.

11 X. Yang, C. R. DeLaney, K. T. Burns, L. C. Elrod, W. Mo, H. Naumann, N. Bhuvanesh, M. B. Hall and M. Y. Darensbourg, *Inorg. Chem.*, 2021, **60**, 7051-7061.

12 X. Peng, J. Han, X. Li, G. Liu, Y. Xu, Y. Peng, S. Nie, W. Li, X. Li, Z. Chen, H. Peng, R. Cao and Y. Fang, *Chem. Commun.*, 2023, **59**, 10777-10780.

13 Q.-W. Yan, L.-W. Wu, Z.-W. Liu, F. Chen, C. Ling, H.-Y. Liu, X.-Y. Xiao and L.-P. Si, *Green Chem.*, 2024, **26**, 4574-4581.

14 E. Ahmad, S. Rai and S. K. Padhi, *Int. J. Hydrogen Energy*, 2019, **44**, 16467-16477.